Report: Spatial formulation for the dynamics of floating rigid bodies[1,2]

Alessandro Giusti[3]

Abstract: The report concerns the dynamic analysis of floating bodies for offshore wind energy purposes. In particular, a spatial formulation for the dynamics of rigid bodies is developed in the framework of the recently developed geometric methods which exploit the structure of Lie-groups to solve directly the equations of motion without the necessity of introducing a parametrization to handle the kinematic compatibility. The dynamic problem is completely formulated with respect to an inertial (fixed) frame, even for the rotational motion. Non-follower and follower loads are therefore characterized, also in terms of associated tangent operators, including the special case of linear transformations of the state variables. The algorithm, implemented according to the formulation developed, is then validated by comparison with available exact analytic solutions in order to verify the capabilities of the model.

1 Introduction

The reduction of greenhouse gas emissions is undoubtedly one of the most important challenges of the twenty-first century. In order to reduce the emissions associated with the traditional sources of energy, i.e. fossil fuels, the exploitation of the so called renewable energy resources gained over the years a primary role and focused the research towards the development of proper as well as efficient technologies. Wind energy is one of the most promising renewable resources. In the last fifteen years it had a significant growth (see Figure 1) becoming the third energy resource in terms of produced power and the first renewable energy resource.

In particular, offshore wind energy is becoming more and more important because of the nature of available sites and the better offshore wind conditions, in terms of higher mean wind speed and less turbulent wind field. The exploitation of deep-water wind energy is always associated with the use of floating platforms that had been evaluated as the most economical support concept [12]. Such kind of structures can undergo large displacements especially during severe sea-states [11, 15]. The design and optimization of offshore wind turbines is a very complex problem of wind-wave-structure interaction which requires the use of advanced numerical tools, as accurate as computationally efficient. In this scenario, the dynamics of rigid bodies (as a floating platform) is of great interest and is analysed in this report in the framework of the recently developed geometric methods [1, 4, 22] by using a complete spatial formulation of the dynamic problem.

Day	Activity
7 Dec 2016	Welcome and visit of the Institut für Stahlbau. Spatial formulation of the dynamic problem and characterization of non-follower and follower loads.
8 Dec 2016	Characterization of linear transformations of the state variables (both non-follower and follower).
9 Dec 2016	Presentation of the research: "On the use of Lie-group geometric methods for the dynamics of moored floating platforms". Implementation of the algorithm.
12 Dec 2016	Visit to the laboratory of the Institut für Stahlbau (Prof. Peter Schaumann). Implementation of the algorithm and debugging.
13 Dec 2016	Visit to the laboratory of the Ludwig-Franzius-Institut für Wasserbau, Ästuar- und Küsteningenieurwesen (Prof. Arndt Hildebrandt). Verification and validation tests: comparison of the numerical solution with the exact analytic solution of a 1D forced damped oscillator.
14 Dec 2016	Verification and validation tests: comparison of the numerical solution with some available exact analytic solutions of 3D rotating bodies.
15 Dec 2016	Comparison of the numerical solutions obtained with alternatives approaches (both mixed and local formulations). Analysis and discussion of the results.
16 Dec 2016	Analysis and discussion of the results.

Table 1: Chronology of the activity.

2 Dynamics of rigid bodies

The dynamic problem of a rigid body consists in establishing the evolution in time of the configuration of the system given the initial and boundary conditions. In the formulation of the dynamic problem, the set of dynamic

[1]This is the report of the Short-Term Scientific Mission (STSM), within the TU1304 WINERCOST Action, carried out by Alessandro Giusti, from the University of Florence, who visited the Leibniz Universität Hannover, Institut für Stahlbau, from December 7th, 2016 to December 16th, 2016, as reported and summarized in Table 1.

[2]This report is an extension of the Doctorate thesis *A nonlinear model for the dynamics of moored floating platforms*, written by the Author. For further discussion on the topics the reader is addressed to the thesis.

[3]Department of Civil and Environmental Engineering, University of Florence, Via di Santa Marta 3, 50139 Florence, Italy.
e-mail: alessandro.giusti@dicea.unifi.it

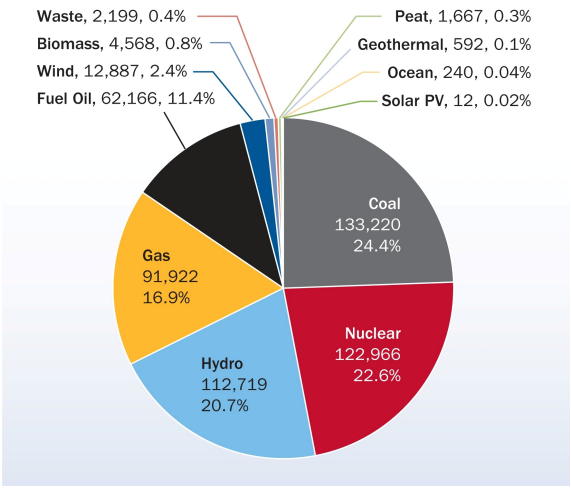

(a) EU power mix in 2000 (MW)

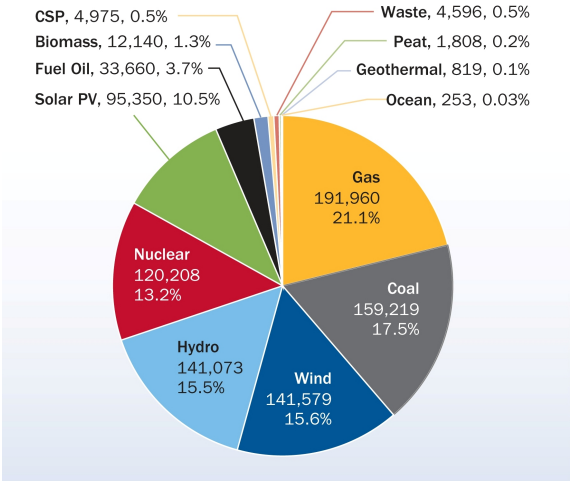

(b) EU power mix in 2015 (MW)

Figure 1: EU power mix [9].

equilibrium equations should be associated with the kinematic equations that relate the velocity of the body with the rotation operator and its time derivative [21]. Such kinematic equations basically define the composition rule for compound translations and rotations on the basis of the velocity representation adopted[4]. Depending on the orthonormal basis used for expressing the physical quantities, different equivalent formulations of the dynamic problem can be obtained.

2.1 Reference frames

The choice of the reference frames used for describing the physical quantities associated with either the translational motion of the center of mass or the rotational motion of the body, can lead to different mathematical formulations of the dynamic problem, formally equivalent, and then to different integration formulas[5]. Let's consider the following two reference frames[6] (see Figure 2):

- inertial (spatial or fixed) reference frame $I = \{O; x, y, z\}$ defined by the orthonormal basis $\mathcal{S} = \{\mathbf{e}_i^I\}$;
- non-inertial (body-attached) reference frame[7] $B = \{G; x', y', z'\}$ defined by the orthonormal basis $\mathcal{M} = \{\mathbf{e}_i^B\}$. This frame can translate and rotate with respect to the fixed frame and an observer solidal with the body-attached frame sees the rigid body fixed. The associated basis changes its orientation according to the motion of the rigid body.

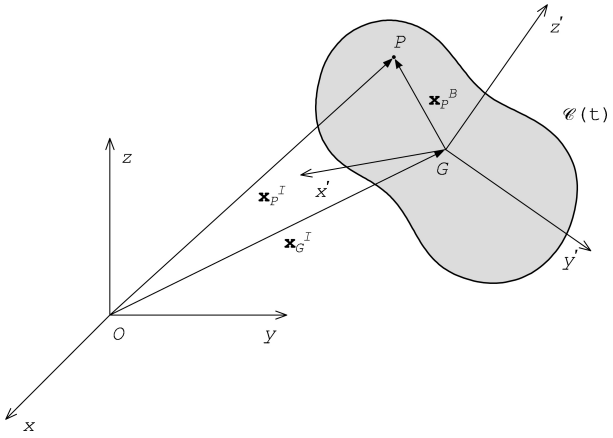

Figure 2: Reference frames.

2.2 Spatial formulation

In the spatial formulation all the physical quantities are expressed with respect to the basis $\mathcal{S}$ which defines the inertial reference frame. The set of equations which solves

[4]The use of either a complete spatial formulation or a mixed formulation or a complete local formulation, i.e. the use of different Lie-groups, is always associated with a specific composition rule, proper of the Lie-group used.

[5]Even if the mathematical formulations are definitely equivalent, the associated time integration algorithms are only approximately equivalent, i.e. the accuracy for a given time step size depends, among others, also on the formulation of the dynamic problem. However, for each formulation, if the time step size tends to zero, also the error tends to zero.

[6]The notation $(\bullet)^{(\diamond),(\circ)}$ indicates a physical quantity $(\bullet)$ observed in the frame $(\diamond)$ and expressed with respect to the basis $(\circ)$, with $(\diamond) = I, B$ and $(\circ) = \mathcal{S}, \mathcal{M}$. Alternatively, if the indication of the reference frame is not significant (for instance for forces and torques), the superscript is limited to the information about the basis, i.e. $(\bullet)^{(\circ)}$.

[7]The origin of the body-attached frame is located at the center of mass of the body. This assumption simplifies the expressions of the linear momentum and angular momentum since all the first moments of volume are zero. However, it is possible to obtain formulations similar to those developed in this work also for generic reference frames.

the dynamic problem is given by[8,9]:

$$\begin{cases} \mathbf{v}_G^{I,\mathcal{S}} = \dot{\mathbf{x}}_G^{I,\mathcal{S}} \\ \dot{\mathbf{R}} = \widetilde{\boldsymbol{\omega}}^{\mathcal{S}}\mathbf{R} \\ m\mathbf{a}_G^{I,\mathcal{S}} = \mathcal{F}^{\mathcal{S}} \\ \mathbf{R}\mathbf{J}^{B,\mathcal{M}}\mathbf{R}^T\dot{\boldsymbol{\omega}}^{\mathcal{S}} + \widetilde{\boldsymbol{\omega}}^{\mathcal{S}}\mathbf{R}\mathbf{J}^{B,\mathcal{M}}\mathbf{R}^T\boldsymbol{\omega}^{\mathcal{S}} = \mathcal{T}_G^{\mathcal{S}} \end{cases}$$

where $\mathbf{J}$ is the tensor of inertia of the body and $\boldsymbol{\omega}$ is the angular velocity. This formulation is usually associated with the Lie-group $\mathbb{R}^3 \times SO(3)$ and the right translation map. Since the inertia tensor depends on the orientation of the body, the dynamic and kinematic problems are always coupled to each other, even in absence of external loads (free rigid body). Only in the very particular case of a sphere (rigid body with a spherical ellipsoid of inertia), if the external loads vanish, the dynamic and kinematic problems are decoupled.

2.3 Mixed formulation

In the mixed formulation[10] the motion of the center of mass is described with respect to the basis $\mathcal{S}$ of the inertial frame whereas the motion about the center of mass is described with respect to the basis $\mathcal{M}$ of the body-attached frame, which changes its orientation during the motion. The set of equations which solves the dynamic problem is given by [21]:

$$\begin{cases} \mathbf{v}_G^{I,\mathcal{S}} = \dot{\mathbf{x}}_G^{I,\mathcal{S}} \\ \dot{\mathbf{R}} = \mathbf{R}\widetilde{\boldsymbol{\omega}}^{\mathcal{M}} \\ m\mathbf{a}_G^{I,\mathcal{S}} = \mathcal{F}^{\mathcal{S}} \\ \mathbf{J}^{B,\mathcal{M}}\dot{\boldsymbol{\omega}}^{\mathcal{M}} + \widetilde{\boldsymbol{\omega}}^{\mathcal{M}}\mathbf{J}^{B,\mathcal{M}}\boldsymbol{\omega}^{\mathcal{M}} = \mathcal{T}_G^{\mathcal{M}} \end{cases}$$

This formulation is usually associated with the Lie-group $\mathbb{R}^3 \times SO(3)$ and the left translation map. The resultant and resultant torque of external forces can be functions of the time and the kinematic quantities, therefore the equations which describes the motion of the center of mass and the motion about the center of mass can be coupled to each other and with the kinematic problem. Only in some particular cases, for instance when the external loads vanish, it is possible to solve the two problems separately and without having to know the actual configuration of the body (independence of kinematic and dynamic problems).

2.4 Local formulation

In the local formulation all the physical quantities are expressed with respect to the basis $\mathcal{M}$ which defines the

[8] In this report it is used a matrix representation of the vector and tensors operations, for further discussions the reader is addressed to the reference [10] among others. In particular, let $\mathbf{p}$ and $\{\mathbf{e}_i\}$ be respectively a vector and a basis of the Euclidean space, the matrix representation of the vector is given by:

$$\mathbf{p} = p_i\mathbf{e}_i = [p_1 \ p_2 \ p_3]^T$$

Given the vectors $\mathbf{p}$ and $\mathbf{w}$ expressed with respect the same basis $\{\mathbf{e}_i\}$, the basic operations in matrix notation are given by:

$$\mathbf{p}\cdot\mathbf{w} = \mathbf{p}^T\mathbf{w}$$
$$\mathbf{p}\otimes\mathbf{w} = \mathbf{p}\mathbf{w}^T$$
$$\mathbf{p}\times\mathbf{w} = \widetilde{\mathbf{p}}\mathbf{w}$$

In the cross product $\mathbf{p}$ is the vector part of $\widetilde{\mathbf{p}}$, i.e. they are linked together by a biunivocal relation, namely [10]:

$$\mathbf{p} = \mathrm{vect}(\widetilde{\mathbf{p}}) = \frac{1}{2}\epsilon_{ijk}\widetilde{p}_{kj}$$
$$\widetilde{\mathbf{p}} = \mathrm{spin}(\mathbf{p}) = -\epsilon_{ijk}p_k$$

where ϵ_{ijk} are the components of the Ricci's tensor (third order tensor) that can be easily determined remembering those three simple rules [5, 10]:

1. $\epsilon_{ijk} = 1$ if ijk is an even permutation (cyclic);
2. $\epsilon_{ijk} = -1$ if ijk is an odd permutation;
3. $\epsilon_{ijk} = 0$ in all the other cases (that is when there is a repeated index).

[9] The rotation is a linear transformation which preserve the distances and the reciprocal orientation between different points of the same body. Rotations are described by a proper orthogonal matrix that depends on three independent parameters. The choice of the set of parameters is not unique and usually relates to the specific issue. Several kinds of parametrization were proposed over the years, which can differ to each other in terms of independence, mathematical form, existence of singularities, computational efficiency, composition low, geometric interpretation, etc. [10]. For instance, nautical angles (or Tait-Bryan or Euler angles) as well as Euler angles are widely used in maritme engineering because of their direct interpretation, whereas quaternions, i.e. a paremeterization with a redundant number of parameters, were introduced to improve the computational effeciency and to prevent singularities (gimbal lock). In the framework of geometric methods, rotations are paramterized by the rotational vector that consists of a set of three independent parameters with an easy geometric interpretation and without any kinematic singularities [10]. The rotational vector is defined as the vector with the same direction of the rotation axis and magnitude equal to the rotation amplitude, namely:

$$\boldsymbol{\psi} = \mathbf{u}\phi$$

The rotation operator can be expressed either in trigonometric form or through the exponential map, and admits a series expansion [1, 5, 10, 13], namely:

$$\mathbf{R} = \mathbf{I} + \frac{\sin\phi}{\phi}\widetilde{\boldsymbol{\psi}} + \frac{1-\cos\phi}{\phi^2}\widetilde{\boldsymbol{\psi}}\widetilde{\boldsymbol{\psi}} = \exp(\widetilde{\boldsymbol{\psi}})$$
$$\mathbf{R} = \mathbf{I} + \widetilde{\boldsymbol{\psi}} + \frac{1}{2!}\widetilde{\boldsymbol{\psi}}^2 + \frac{1}{3!}\widetilde{\boldsymbol{\psi}}^3 + \cdots + \frac{1}{n!}\widetilde{\boldsymbol{\psi}}^n$$

where $\phi = \sqrt{\boldsymbol{\psi}^T\boldsymbol{\psi}}$. The tangent operator and its series expansion, associated with the rotational vector representation, are given by [1, 5, 10]:

$$\mathbf{T}(\boldsymbol{\psi}) = \mathbf{I} + \frac{\cos\phi - 1}{\phi^2}\widetilde{\boldsymbol{\psi}} + \left(1 - \frac{\sin\phi}{\phi}\right)\frac{\widetilde{\boldsymbol{\psi}}\widetilde{\boldsymbol{\psi}}}{\phi^2}$$
$$\mathbf{T}(\boldsymbol{\psi}) = \mathbf{I} - \frac{1}{2!}\widetilde{\boldsymbol{\psi}} + \frac{1}{3!}\widetilde{\boldsymbol{\psi}}^2 + \cdots + \frac{(-1)^n}{(n+1)!}\widetilde{\boldsymbol{\psi}}^n$$

Note that the apparent singularity in the previous equations for $\phi = 0$, can be removed by noticing that both the expressions in the neighbourhood of $\boldsymbol{\psi} = \mathbf{0}$ tend to the identity matrix. The inverse function of the rotation operator, called *logarithmic map*, returns the rotational vector $\boldsymbol{\psi}$ associated with the rotational operator $\mathbf{R}(\boldsymbol{\psi})$, namely:

$$\widetilde{\boldsymbol{\psi}} = \frac{\vartheta}{2\sin\vartheta}(\mathbf{R} - \mathbf{R}^T) \qquad , \qquad \vartheta = \cos^{-1}\left[\frac{\mathrm{tr}(\mathbf{R}) - 1}{2}\right]$$

[10] If the origin of the body-attached frame is located in the center of mass of the body (barycentric frame), this approach ensures the simplest form of the dynamic problem. In fact the motion of the center of mass is described by the second Newton's law whereas the motion about the center of mass is described by the Euler's equations.

body-attached frame. The set of equations which solves the dynamic problem is given by [21]:

$$\begin{cases} \mathbf{v}_G^{I,\mathcal{S}} = \mathbf{R}\mathbf{v}_G^{I,\mathcal{M}} \\ \dot{\mathbf{R}} = \mathbf{R}\widetilde{\boldsymbol{\omega}}^{\mathcal{M}} \\ m\dot{\mathbf{v}}_G^{I,\mathcal{M}} + m\widetilde{\boldsymbol{\omega}}^{\mathcal{M}}\mathbf{v}_G^{I,\mathcal{M}} = \mathcal{F}^{\mathcal{M}} \\ \mathbf{J}^{B,\mathcal{M}}\dot{\boldsymbol{\omega}}^{\mathcal{M}} + \widetilde{\boldsymbol{\omega}}^{\mathcal{M}}\mathbf{J}^{B,\mathcal{M}}\boldsymbol{\omega}^{\mathcal{M}} = \mathcal{T}_G^{\mathcal{M}} \end{cases}$$

This formulation is usually associated with the Lie-group $SE(3)$. If the external loads vanish (free rigid body), the dynamic equilibrium equations are independent from the kinematic ones, i.e. they can be solved without having to know the actual configuration of the body [21]. However, in the most general case of forced motions, the dynamic and kinematic problems are coupled to each other.

2.5 Linear operators

Let's focus on the spatial formulation. Let $\hat{\mathbf{q}} = [\mathbf{x}_G^{I,\mathcal{S}}; \boldsymbol{\psi}]$ be the state position vector[11], collecting the position vector of the center of mass and the rotational vector, let $\hat{\mathbf{v}} = [\mathbf{v}_G^{I,\mathcal{S}}; \boldsymbol{\omega}^{\mathcal{S}}]$ be the state velocity vector, collecting the velocity vector of the center of mass and the angular velocity vector, let $\hat{\dot{\mathbf{v}}} = [\mathbf{a}_G^{I,\mathcal{S}}; \dot{\boldsymbol{\omega}}^{\mathcal{S}}]$ be the state acceleration vector, collecting the acceleration vector of the center of mass and the angular acceleration vector. These three quantities can be regarded as state variables and completely describe the rigid-body motion. The dynamic equilibrium equations can be written in terms of such state variables and naturally define the residual vector $\hat{\mathbf{r}}$, namely:

$$\hat{\mathbf{r}} = \begin{bmatrix} m\mathbf{I}_3 & \mathbf{0}_{3\times3} \\ \mathbf{0}_{3\times3} & \mathbf{R}\mathbf{J}^{B,\mathcal{M}}\mathbf{R}^T \end{bmatrix} \hat{\dot{\mathbf{v}}} + \begin{bmatrix} \mathbf{0}_{3\times1} \\ \widetilde{\hat{\mathbf{v}}}_{4:6}\mathbf{R}\mathbf{J}^{B,\mathcal{M}}\mathbf{R}^T\hat{\mathbf{v}}_{4:6} \end{bmatrix} + - \begin{bmatrix} \mathcal{F}^{\mathcal{S}}(\hat{\mathbf{q}}, \hat{\mathbf{v}}, \hat{\dot{\mathbf{v}}}, t) \\ \mathcal{T}_G^{\mathcal{S}}(\hat{\mathbf{q}}, \hat{\mathbf{v}}, \hat{\dot{\mathbf{v}}}, t) \end{bmatrix} = \mathbf{0}_{6\times1} \tag{1}$$

The linearization of the Equation (1) with respect to the state variables defines the tangent (stiffness, damping and mass) operators, namely[12]:

$$\mathbf{K}^t \cdot \Delta\hat{\mathbf{q}} = D_{\mathbf{q}}\hat{\mathbf{r}} \cdot \Delta\hat{\mathbf{q}} \tag{2}$$

$$\mathbf{C}^t \cdot \Delta\hat{\mathbf{v}} = D_{\mathbf{v}}\hat{\mathbf{r}} \cdot \Delta\hat{\mathbf{v}} \tag{3}$$

$$\mathbf{M}^t \cdot \Delta\hat{\dot{\mathbf{v}}} = D_{\dot{\mathbf{v}}}\hat{\mathbf{r}} \cdot \Delta\hat{\dot{\mathbf{v}}} \tag{4}$$

[11] Even if the state variable associated with the configuration of the body is expressed as a vector $\hat{\mathbf{q}} \in \mathbb{R}^6$, do not confuse the nature of the rotational vector $\boldsymbol{\psi}$ which is a parametrization of the rotation operator $\mathbf{R} \in SO(3)$. The state position vector should therefore be treated as an element $\hat{q}$ of the Lie-group $\mathbb{R}^3 \times SO(3)$, namely $\hat{q} \in \mathbb{R}^3 \times SO(3)$.

[12] The directional derivative with respect to the position state variable $\hat{\mathbf{q}} = [\mathbf{x}_G^{I,\mathcal{S}}; \boldsymbol{\psi}]$ requires somehow attention because of the nature of the rotational vector $\boldsymbol{\psi}$ which represents elements of the special orthogonal group of finite rotations $SO(3)$. In the framework of the spatial formulation, compound rotations are defined by the right translation map. Because of the structure of the algorithm [1], the directional derivative of the rotation is computed with respect to the increment $\boldsymbol{\theta}^{\mathcal{S}}$ of the current rotation operator $\mathbf{R}(\boldsymbol{\psi})$ which is related to the increment of the rotational vector through the tangent operator, namely $\boldsymbol{\theta}^{\mathcal{S}} = [\mathbf{T}(\boldsymbol{\psi})]^T\delta\boldsymbol{\psi}$. By contrast, the position vector of the center of mass does not introduce any significant issue.

2.6 Rotation derivatives

The rotation operator can be seen as a linear transformation and, in the dynamics of rigid bodies, it is usually applied to vectors or to a composition of matrices and vectors, i.e. to another vector. Hence, the derivative of the resulting vector with respect to the rotational vector (state variable) becomes of particular interest. Let $\mathbf{z}$ be a vector[13]:

$$\mathbf{R}^T(\boldsymbol{\psi})\mathbf{z}^{\mathcal{S}} \quad , \quad D(\mathbf{R}^T\mathbf{z}^{\mathcal{S}}) \cdot \widetilde{\boldsymbol{\theta}}^{\mathcal{S}} = \mathbf{R}^T\widetilde{\mathbf{z}}^{\mathcal{S}}\boldsymbol{\theta}^{\mathcal{S}} \tag{5}$$

$$\mathbf{R}(\boldsymbol{\psi})\mathbf{z}^{\mathcal{M}} \quad , \quad D(\mathbf{R}\mathbf{z}^{\mathcal{M}}) \cdot \widetilde{\boldsymbol{\theta}}^{\mathcal{S}} = -\widetilde{[\mathbf{R}\mathbf{z}^{\mathcal{M}}]}\boldsymbol{\theta}^{\mathcal{S}} \tag{6}$$

3 Algorithm

The spatial differential problem (see Section 2.2) that describes the dynamics of a rigid body in the Euclidean space (six degrees of freedom) is solved with an efficient Lie-group time integrator based on the geometric method developed in [1, 2, 3, 4]. The time integration scheme is an extension of the generalized-α method for Lie-groups [4]. At each time step, the equations are solved for all the variables on the basis of their values at the previous time step, by means of a Newton-Raphson scheme which involves the linearization of the nonlinear problem around the current configuration by means of the tangent operators. The algorithm operates directly in the Lie-group $\mathbb{R}^3 \times SO(3)$ and rotations are parameterized by the rotational vector.

Given the state variables $\hat{\mathbf{q}}$, $\hat{\mathbf{v}}$ and $\hat{\dot{\mathbf{v}}}$ at time t_n, the state variables at time t_{n+1} can be computed with the Algorithm 1. For further discussions on other possible numerical approaches the reader is addressed to the references [5, 7, 6, 13, 14, 18, 19, 20, 23].

3.1 Mappings

The algorithms proposed in [1] are a family of Lie-group time integrators defined by the mappings used for updating the state variable $\hat{\mathbf{q}}$, i.e. $\hat{\mathbf{q}}_{n+1} = \varphi_h(\hat{\mathbf{q}}_n, \hat{\mathbf{v}}_n, \mathbf{a}_n, \mathbf{a}_{n+1})$. The use of a complete spatial formulation and the consequent introduction of the right translation map to define compound rotations [13], require a modification of the original mappings. In particular, the new mappings $\varphi^1_{h*}(\hat{\mathbf{q}}_n, \mathbf{v}_n, \mathbf{a}_n)$ and $\varphi^1_{hx}(\hat{\mathbf{v}}_n, \mathbf{a}_n, \mathbf{a}_{n+1})$, are given by:

$$\hat{\mathbf{q}}_{n+1} = \varphi^1_h(\hat{\mathbf{q}}_n, \hat{\mathbf{v}}_n, \mathbf{a}_n, \mathbf{a}_{n+1}) = \exp(\widetilde{\varphi}^1_{hx}) \circ \varphi^1_{h*} \tag{7}$$

$$\varphi^1_{h*} = \hat{\mathbf{q}}_n \tag{8}$$

$$\varphi^1_{hx} = h\hat{\mathbf{v}}_n + h^2(0.5 - \beta)\mathbf{a}_n + \beta h^2\mathbf{a}_{n+1} \tag{9}$$

Note that in the previous equations the exponential map, $\exp(\bullet) \in \mathbb{R}^3 \times SO(3)$, of the quantity $(\bullet) \in \mathbb{R}^6$ is given by:

[13] These derivatives can easily be verified. Let $\delta\boldsymbol{\psi}$ be an infinitesimal rotation belonging to the tangent space at the identity, for any finite rotation $\boldsymbol{\psi}$ and any vector $\mathbf{z}$ it follows that:

$$[\mathbf{R}^T(\boldsymbol{\psi} + \delta\boldsymbol{\psi}) - \mathbf{R}^T(\boldsymbol{\psi})]\mathbf{z} \approx \mathbf{R}^T(\boldsymbol{\psi})\widetilde{\mathbf{z}}\mathbf{T}^T(\boldsymbol{\psi})\delta\boldsymbol{\psi}$$

$$[\mathbf{R}(\boldsymbol{\psi} + \delta\boldsymbol{\psi}) - \mathbf{R}(\boldsymbol{\psi})]\mathbf{z} \approx -\widetilde{[\mathbf{R}(\boldsymbol{\psi})\mathbf{z}]}\mathbf{T}^T(\boldsymbol{\psi})\delta\boldsymbol{\psi}$$

Algorithm 1: Scheme (single time step) for the solution of the spatial formulation of the dynamic problem.

input : h, α_f, α_m, β, γ, tol, n_{max}, m, $\mathbf{J}$, $\mathbf{g}$, $\hat{\mathbf{q}}_n$, $\hat{\mathbf{v}}_n$, $\hat{\dot{\mathbf{v}}}_n$, $\mathbf{a}_n$, $\mathbf{F}^{(\bullet)}$, $\mathbf{T}^{(\bullet)}$, $\mathbf{A}^{(\bullet)}$, $\mathbf{B}^{(\bullet)}$, ...

output: $\hat{\mathbf{q}}_{n+1}$, $\hat{\mathbf{v}}_{n+1}$, $\hat{\dot{\mathbf{v}}}_{n+1}$, $\mathbf{a}_{n+1}$

$\beta' = \frac{1-\alpha_m}{\beta h^2(1-\alpha_f)}$;
$\gamma' = \frac{\gamma}{\beta h}$;
$\hat{\dot{\mathbf{v}}}_{n+1} = \mathbf{0}$;
$\mathbf{a}_{n+1} = \frac{\alpha_f \hat{\mathbf{v}}_n - \alpha_m \mathbf{a}_n}{1-\alpha_m}$;
$\hat{\mathbf{v}}_{n+1} = \hat{\mathbf{v}}_n + h(1-\gamma)\mathbf{a}_n + \gamma h \mathbf{a}_{n+1}$;
$\mathbf{q}^* = \varphi^a_{h^*}(\hat{\mathbf{q}}_n, \hat{\mathbf{v}}_n, \mathbf{a}_n, h, \beta) \quad , \quad a = 1,2,3;$
$\mathbf{y} = \varphi^a_{hx}(\hat{\mathbf{v}}_n, \mathbf{a}_n, \mathbf{a}_{n+1}, h, \beta) \quad , \quad a = 1,2,3;$
for $i \leftarrow 1$ **to** n_{max} **do**
  $\hat{\mathbf{q}}_{n+1,1:3} = \mathbf{x}_{n+1} = \mathbf{q}^*_{1:3} + \mathbf{y}_{1:3}$;
  $\hat{\mathbf{q}}_{n+1,4:6} = \boldsymbol{\psi}_{n+1} = \log_{\mathbf{R}}\big[\mathbf{R}(\mathbf{y}_{4:6})\mathbf{R}(\mathbf{q}^*_{4:6})\big]$;
  $\hat{(\diamond)}^{(\bullet)} = \hat{(\diamond)}^{(\bullet)}(\hat{\mathbf{q}}_{n+1}, t_{n+1}) \quad , \quad (\diamond) = \mathbf{F}, \mathbf{T}, \mathbf{A}, \mathbf{B};$
  $\mathbf{res} = \hat{\mathbf{r}}(\hat{\mathbf{q}}_{n+1}, \hat{\mathbf{v}}_{n+1}, \hat{\dot{\mathbf{v}}}_{n+1}, t_{n+1})$;
  if $||\mathbf{res}|| < tol$ **then**
    break;
  end
  $\mathbf{M}^t = \mathbf{M}^t(\hat{\mathbf{q}}_{n+1}, \hat{\mathbf{v}}_{n+1}, \hat{\dot{\mathbf{v}}}_{n+1}, t_{n+1})$;
  $\mathbf{C}^t = \mathbf{C}^t(\hat{\mathbf{q}}_{n+1}, \hat{\mathbf{v}}_{n+1}, \hat{\dot{\mathbf{v}}}_{n+1}, t_{n+1})$;
  $\mathbf{K}^t = \mathbf{K}^t(\hat{\mathbf{q}}_{n+1}, \hat{\mathbf{v}}_{n+1}, \hat{\dot{\mathbf{v}}}_{n+1}, t_{n+1})$;
  $\mathbf{T}^\dagger_{1:3\times 1:3} = \mathbf{I}_3$;
  $\mathbf{T}^\dagger_{4:6\times 4:6} = \mathbf{I}_3 - \frac{cos\phi - 1}{\phi^2}\widetilde{\mathbf{y}}_{4:6} + \left(1 - \frac{sin\phi}{\phi}\right)\frac{\widetilde{\mathbf{y}}_{4:6}\widetilde{\mathbf{y}}_{4:6}}{\phi^2}$;
  $\mathbf{S}_t = \beta' \mathbf{M}^t + \gamma' \mathbf{C}^t + \mathbf{K}^t \mathbf{T}^\dagger$;
  $\Delta\mathbf{y} = -\mathbf{S}_t^{-1}\mathbf{res}$;
  $\mathbf{y} = \mathbf{y} + \Delta\mathbf{y}$;
  $\hat{\mathbf{v}}_{n+1} = \hat{\mathbf{v}}_{n+1} + \gamma' \Delta\mathbf{y}$;
  $\hat{\dot{\mathbf{v}}}_{n+1} = \hat{\dot{\mathbf{v}}}_{n+1} + \beta' \Delta\mathbf{y}$;
end
$\mathbf{a}_{n+1} = \mathbf{a}_{n+1} + \frac{1-\alpha_f}{1-\alpha_m}\hat{\dot{\mathbf{v}}}_{n+1}$;

$$\exp(\widetilde{\bullet}) = \begin{bmatrix} (\bullet)_{1:3} \\ \exp_{SO(3)}(\widetilde{\bullet}_{4:6}) \end{bmatrix} \tag{10}$$

The composition rules of the quantities $[\mathbf{x}^a; \mathbf{R}^a], [\mathbf{x}^b; \mathbf{R}^b] \in \mathbb{R}^3 \times SO(3)$ is given by:

$$[\mathbf{x}^a; \mathbf{R}^a] \circ [\mathbf{x}^b; \mathbf{R}^b] = \begin{bmatrix} \mathbf{x}^a + \mathbf{x}^b \\ \mathbf{R}^a \mathbf{R}^b \end{bmatrix} \tag{11}$$

4 Inertial loads

According to the D'Alembert's principle, an accelerating body can be transformed into an equivalent static system by means of the so called inertial loads[14], namely:

$$\mathbf{F}^{\mathcal{S}}_G = -m\hat{\dot{\mathbf{v}}}_{1:3} \tag{12}$$

$$\mathbf{T}^{\mathcal{S}}_G = -\mathbf{J}^{B,\mathcal{S}}\hat{\dot{\mathbf{v}}}_{4:6} - \hat{\mathbf{v}}_{4:6} \times \mathbf{J}^{B,\mathcal{S}}\hat{\mathbf{v}}_{4:6} \tag{13}$$

[14]The inertial loads are equivalent external forces and torques associated with the accelerating masses.

where $\mathbf{J}^{B,\mathcal{S}} = \mathbf{R}\mathbf{J}^{B,\mathcal{M}}\mathbf{R}^T$. The tangent operators associated with the inertial loads are:

$$\mathbf{M}^t_{1:3\times 1:3} = m\mathbf{I}_3 \tag{14}$$

$$\mathbf{M}^t_{4:6\times 4:6} = \mathbf{R}\mathbf{J}^{B,\mathcal{M}}\mathbf{R}^T \tag{15}$$

$$\mathbf{C}^t_{4:6\times 4:6} = \widetilde{\hat{\mathbf{v}}}_{4:6}\mathbf{J}^{B,\mathcal{S}} - \widetilde{(\mathbf{J}^{B,\mathcal{S}}\hat{\mathbf{v}}_{4:6})} \tag{16}$$

$$\begin{aligned}\mathbf{K}^t_{4:6\times 4:6} = &-\widetilde{\big(\mathbf{J}^{B,\mathcal{S}}\hat{\dot{\mathbf{v}}}_{4:6}\big)} + \mathbf{J}^{B,\mathcal{S}}\widetilde{\hat{\dot{\mathbf{v}}}}_{4:6} + \\ &- \widetilde{\hat{\mathbf{v}}}_{4:6}\widetilde{\big(\mathbf{J}^{B,\mathcal{S}}\hat{\mathbf{v}}_{4:6}\big)} + \widetilde{\hat{\mathbf{v}}}_{4:6}\mathbf{J}^{B,\mathcal{S}}\widetilde{\hat{\mathbf{v}}}_{4:6}\end{aligned} \tag{17}$$

5 Non-follower loads

A load is said non-follower if its orientation does not depend on the orientation of the body. The classic example is the gravity force which is always directed downward regardless the configuration of the body. The components of a non-follower load, both force and torque, are naturally referred to the basis $\mathcal{S}$ of the inertial (fixed) frame, i.e. $\mathbf{F}^{nf}, \mathbf{T}^{nf} \in \{\mathcal{S}\}$. In the spatial formulation, non-follower loads are rather simple to handle because they are already oriented according to the basis used in the formulation of the dynamic problem. Only the torque associated with eccentric forces introduces some issues because the arm of the load is generally defined with respect to the body-attached frame, i.e. the basis $\mathcal{M}$.

5.1 Force

Let $\mathbf{F}^{nf}_P$ be a non-follower force, applied in the location (point) P of the rigid body, which can depend on time but not on the state variables. Its contribution to the loads acting on the system in the spatial formulation is given by:

$$\hat{\mathbf{F}} = \mathbf{F}^{\mathcal{S}}_G = \mathbf{F}^{nf}_P \tag{18}$$

$$\hat{\mathbf{T}} = \mathbf{T}^{\mathcal{S}}_G = \widetilde{\mathbf{x}}^{B,\mathcal{S}}_P \mathbf{F}^{nf}_P = \mathbf{R}\widetilde{\mathbf{x}}^{B,\mathcal{M}}_P \mathbf{R}^T \mathbf{F}^{nf}_P \tag{19}$$

The tangent operator associated with the non-follower force is given by:

$$\mathbf{K}^t_{4:6\times 4:6} = \widetilde{\big(\mathbf{R}\widetilde{\mathbf{x}}^{B,\mathcal{M}}_P \mathbf{R}^T \mathbf{F}^{nf}_P\big)} - \mathbf{R}\widetilde{\mathbf{x}}^{B,\mathcal{M}}_P \mathbf{R}^T \widetilde{\mathbf{F}}^{nf}_P \tag{20}$$

5.2 Torque

Let $\mathbf{T}^{nf}_P$ be a non-follower moment, applied in the location (point) P of the rigid body, which can depend on time but not on the state variables. Its contribution to the loads acting on the system in the spatial formulation is given by:

$$\hat{\mathbf{F}} = \mathbf{F}^{\mathcal{S}}_G = \mathbf{0}_{3\times 1} \tag{21}$$

$$\hat{\mathbf{T}} = \mathbf{T}^{\mathcal{S}}_G = \mathbf{T}^{nf}_P \tag{22}$$

The non-follower torque does not contribute to the tangent operators of the system.

5.3 Linear transformations

An interesting case refers to loads which can be modelled as linear transformations of the state variables $\mathbf{q}$, $\mathbf{v}$, $\dot{\mathbf{v}}$, defined with respect to the basis $\mathcal{S}$ of the inertial frame, i.e. non-follower transformations[15]. The matrices associated with the linear transformations should be properly converted on the basis of the spatial formulation adopted.

Let $\mathbf{A}$ be the square matrix of order six associated with a non-follower linear transformation of the state variables $[(\bullet)^{\mathcal{S}};(\diamond)^{\mathcal{S}}]$, where $(\bullet)$ and $(\diamond)$ are respectively the variables related to the translational and rotational motions, namely:

$$\left[\begin{array}{c}\mathbf{F}_G^{\mathcal{S}}\\ \mathbf{T}_G^{\mathcal{S}}\end{array}\right] = -\mathbf{A}\left[\begin{array}{c}(\bullet)^{\mathcal{S}}\\ (\diamond)^{\mathcal{S}}\end{array}\right] \tag{23}$$

The non-follower transformation $\mathbf{A}$ associated with the spatial formulation, indicated with the notation $\hat{\mathbf{A}}$, is given by:

$$\left[\begin{array}{c}\mathbf{F}_G^{\mathcal{S}}\\ \mathbf{T}_G^{\mathcal{S}}\end{array}\right] = -\hat{\mathbf{A}}\left[\begin{array}{c}(\bullet)^{\mathcal{S}}\\ (\diamond)^{\mathcal{S}}\end{array}\right] \tag{24}$$

$$\hat{\mathbf{A}} = \mathbf{A} \tag{25}$$

In this case, the transformation does not need to be converted since it is already expressed with respect to the basis of the inertial reference frame. As a consequence, the tangent operators associated with the transformation are simply given by the matrix $\hat{\mathbf{A}}$.

6 Follower loads

A load is said follower if it is dragged by the body during the motion (it rotates with the body). The components of a follower load, both force and torque, are naturally referred to the basis $\mathcal{M}$ of the non-inertial frame, i.e. $\mathbf{F}^f, \mathbf{T}^f \in \{\mathcal{M}\}$. Because of the spatial formulation, the components of follower loads should be properly modified in order to be coherent with the basis used in the formulation of the dynamic problem.

6.1 Force

Let $\mathbf{F}_P^f$ be a follower force, applied in the location (point) P of the rigid body, which can depend on time but not on the state variables. Its contribution to the loads acting on the system in the spatial formulation is given by:

$$\hat{\mathbf{F}} = \mathbf{F}_G^{\mathcal{S}} = \mathbf{R}\mathbf{F}_P^f \tag{26}$$

$$\hat{\mathbf{T}} = \mathbf{T}_G^{\mathcal{S}} = \mathbf{R}\tilde{\mathbf{x}}_P^{B,\mathcal{M}}\mathbf{F}_P^f \tag{27}$$

[15]For instance, in the case of floating bodies in the framework of the linear theory, the hydrodynamic operators (added mass and damping matrices) as well as the hydrostatic stiffness matrix, are usually defined as non-follower linear transformations of the state variables.

The tangent operator associated with the follower force is given by:

$$\mathbf{K}_{1:3\times 4:6}^t = \widetilde{\left(\mathbf{R}\mathbf{F}_P^f\right)} \tag{28}$$

$$\mathbf{K}_{4:6\times 4:6}^t = \widetilde{\left(\mathbf{R}\tilde{\mathbf{x}}_P^{B,\mathcal{M}}\mathbf{F}_P^f\right)} \tag{29}$$

6.2 Torque

Let $\mathbf{T}_P^f$ be a follower moment, applied in the location (point) P of the rigid body, which can depend on time but not on the state variables. Its contribution to the loads acting on the system in the spatial formulation is given by:

$$\hat{\mathbf{F}} = \mathbf{F}_G^{\mathcal{S}} = \mathbf{0}_{3\times 1} \tag{30}$$

$$\hat{\mathbf{T}} = \mathbf{T}_G^{\mathcal{S}} = \mathbf{R}\mathbf{T}_P^f \tag{31}$$

The tangent operator associated with the follower torque is given by:

$$\mathbf{K}_{4:6\times 4:6}^t = \widetilde{\left(\mathbf{R}\mathbf{T}_P^f\right)} \tag{32}$$

6.3 Linear transformations

Similar to the case introduced in the previous section, an interesting case refers to loads which can be modelled as linear transformations of the state variables $\mathbf{q}$, $\mathbf{v}$, $\dot{\mathbf{v}}$, defined with respect to the basis $\mathcal{M}$ of the body-attached frame, i.e. follower transformations. The matrices associated with the linear transformations should be properly converted on the basis of the spatial formulation adopted.

Let $\mathbf{B}$ be the square matrix of order six associated with a follower linear transformation of the state variables $[(\bullet)^{\mathcal{M}};(\diamond)^{\mathcal{M}}]$, where $(\bullet)$ and $(\diamond)$ are respectively the variables related to the translational and rotational motions, namely:

$$\left[\begin{array}{c}\mathbf{F}_G^{\mathcal{M}}\\ \mathbf{T}_G^{\mathcal{M}}\end{array}\right] = -\mathbf{B}\left[\begin{array}{c}(\bullet)^{\mathcal{M}}\\ (\diamond)^{\mathcal{M}}\end{array}\right] \tag{33}$$

The follower transformation $\mathbf{B}$ associated with the spatial formulation, indicated with the notation $\hat{\mathbf{B}}$, is given by:

$$\left[\begin{array}{c}\mathbf{F}_G^{\mathcal{S}}\\ \mathbf{T}_G^{\mathcal{S}}\end{array}\right] = -\hat{\mathbf{B}}\left[\begin{array}{c}(\bullet)^{\mathcal{S}}\\ (\diamond)^{\mathcal{S}}\end{array}\right] \tag{34}$$

$$\hat{\mathbf{B}} = \left[\begin{array}{cc}\mathbf{R}\mathbf{B}_{1:3\times 1:3}\mathbf{R}^T & \mathbf{R}\mathbf{B}_{1:3\times 4:6}\mathbf{R}^T\\ \mathbf{R}\mathbf{B}_{4:6\times 1:3}\mathbf{R}^T & \mathbf{R}\mathbf{B}_{4:6\times 4:6}\mathbf{R}^T\end{array}\right] \tag{35}$$

The tangent operators associated with the transformation are given by the matrix $\hat{\mathbf{B}}$ itself plus the tangent stiffness related to the change of orientation of the body, namely:

$$\begin{aligned}\mathbf{K}_{1:3\times 4:6}^t = &-\widetilde{\left[\hat{\mathbf{B}}_{1:3\times 1:3}(\bullet)^{\mathcal{S}}\right]} + \hat{\mathbf{B}}_{1:3\times 1:3}\widetilde{(\bullet)}^{\mathcal{S}} + \\ &-\widetilde{\left[\hat{\mathbf{B}}_{1:3\times 4:6}(\diamond)^{\mathcal{S}}\right]} + \hat{\mathbf{B}}_{1:3\times 4:6}\widetilde{(\diamond)}^{\mathcal{S}}\end{aligned} \tag{36}$$

$$\begin{aligned}\mathbf{K}_{4:6\times 4:6}^t = &-\widetilde{\left[\hat{\mathbf{B}}_{4:6\times 1:3}(\bullet)^{\mathcal{S}}\right]} + \hat{\mathbf{B}}_{4:6\times 1:3}\widetilde{(\bullet)}^{\mathcal{S}} + \\ &-\widetilde{\left[\hat{\mathbf{B}}_{4:6\times 4:6}(\diamond)^{\mathcal{S}}\right]} + \hat{\mathbf{B}}_{4:6\times 4:6}\widetilde{(\diamond)}^{\mathcal{S}}\end{aligned} \tag{37}$$

7 Validation tests

In order to prove the effectiveness of the approach, the numerical model, based on the Lie-group algorithm developed according to the spatial formulation, is tested on a number of models for which an exact analytic solution exists. Unluckily, exact analytic solutions are available only for few simple cases, as the one degree-of-freedom oscillators (free, damped and forced) or the rotating sphere in the Euclidean space. Of course, the most practical problems are much more complex and require a numerical solution.

7.1 Sphere with follower torque

Let's consider a rigid body with spherical ellipsoid of inertia subjected to a constant follower torque[16] in the very particular case of absence of the gravity acceleration field, i.e. absence of external net forces (weight). The features of system and loads are reported in Table 2. Since there are not external net forces applied on the body, the system rotates about the center of mass (which does not translate). This example allows us to validate the part of the code which deals with finite rotations by means of a direct comparison with the exact analytic solution developed in [16][17].

environment		
gravity acceleration, g	0.00	m/s^2
rigid body		
inertia, $\mathbf{J}$	diag(3 3 3)	kg·m^2
reference point, $\mathbf{x}_P^{B,\mathcal{M}}$	$[0\ 0\ -0.6]^T$	m
loads		
torque, $\mathbf{T}_G^f$	$[0\ 0\ 30]^T$	N·m
initial conditions		
displacement, $\boldsymbol{\psi}\|_{t=0}$	$[0\ 0\ 0]^T$	rad
velocity, $\hat{\mathbf{v}}\|_{t=0}$	$[0\ 0\ 0\ 10\ 15\ 20]^T$	m/s|rad/s

Table 2: Sphere with follower torque: parameters used for the analysis.

7.1.1 Error evaluation

The numerical and analytic solutions are compared in terms of mean absolute error evaluated on the displacement of the reference point $\mathbf{x}_P^{B,\mathcal{M}}$ at a set of specified times t_i, namely [1]:

$$\text{error} = \frac{1}{n_{step}} \sum_{i=1}^{n_{step}} ||\mathbf{x}_P^{B,\mathcal{S}(\text{num})}(t_i) - \mathbf{x}_P^{B,\mathcal{S}(\text{ref})}(t_i)|| \quad (38)$$

$$\mathbf{x}_P^{B,\mathcal{S}}(t_i) = \mathbf{R}\big[\boldsymbol{\psi}(t_i)\big]\mathbf{x}_P^{B,\mathcal{M}}(t_i) \quad (39)$$

[16]The dynamic problem addressed in this section is the same studied in [1] and it is used as a benchmark.

[17]This is one of the few cases (see also the next section) for which an analytic solution is available for a three dimensional rotational motion.

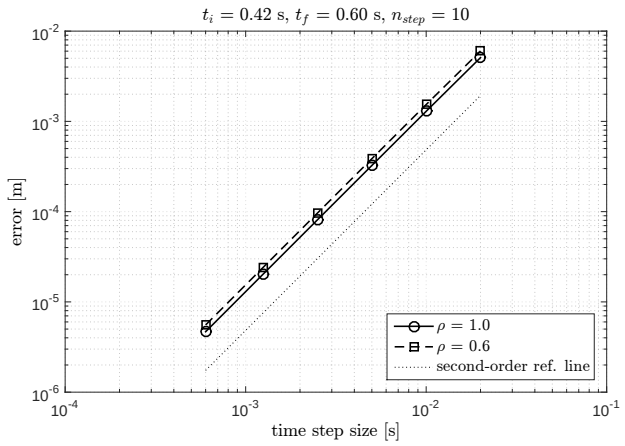

(a) error

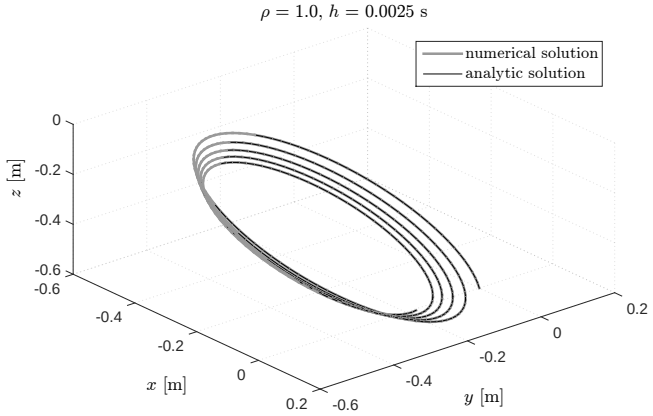

(b) trajectory

Figure 3: Sphere with follower torque: comparison between the numerical solution and the exact analytic solution.

7.1.2 Results

The algorithm (see Figure 3), as expected, exhibits a second-order convergence with respect to the time step size. Coherently with the external torque and the initial conditions, the reference point depicts a curved trajectory about a variable axis. The numerical damping[18] does not significantly affect the accuracy of the numerical solution even if the larger the damping the larger the error.

7.1.3 Remarks

The error exhibits a second-order accuracy similar to the results reported in [1], where the same system is analysed with the same initial and contour conditions but using an algorithm based on the mixed formulation. Regardless the numerical damping, it is possible to get a good level of accuracy for a wide range of time step sizes.

[18]In the present work, the numerical damping, and then the algorithmic parameters, is controlled by the parameter ρ according to the formulation developed in [8].

7.2 Axially symmetric rigid body

Let's consider an axially symmetric rigid body subjected to a constant follower torque about the axis of symmetry in the very particular case of absence of the gravity acceleration field, i.e. absence of external net forces (weight). The features of system and loads are reported in Table 3. Since there are not external net forces applied on the body, the system rotates about the center of mass (which does not translate). The exact analytic solution is developed in [17].

environment		
gravity acceleration, g	0.00	m/s^2
rigid body		
inertia, $\mathbf{J}$	diag(20 20 7)	kg·m^2
reference point, $\mathbf{x}_P^{B,\mathcal{M}}$	$[0\ 0\ -0.6]^T$	m
loads		
torque, $\mathbf{T}_G^f$	$[0\ 0\ 30]^T$	N·m
initial conditions		
displacement, $\boldsymbol{\psi}\|_{t=0}$	$[0\ 0\ 0]^T$	rad
velocity, $\hat{\mathbf{v}}\|_{t=0}$	$[0\ 0\ 0\ 1.0\ 2.0\ 3.0]^T$	m/s|rad/s

Table 3: Axially symmetric rigid body: parameters used for the analysis.

7.2.1 Results

The numerical and analytic solutions are compared in terms of mean absolute error evaluated on the displacement of the reference point $\mathbf{x}_P^{B,\mathcal{M}}$ at a set of specified times t_i, by using the Equation (38). The numerical error (see Figure 4(a)) exhibit a second-order convergence with respect to the time step size. The numerical damping slightly modifies the accuracy of the algorithm, in particular, the larger the damping the larger the error. Moreover, if the system rotates faster (see Figure 4(b), initial velocity doubled), the error is larger. Therefore, in the case of very large velocities, only small time step sizes can guarantee high levels of accuracy.

7.2.2 Remarks

The algorithm based on the spatial formulation can properly describe the motion of a rotating body with a satisfying level of accuracy which depends on both the numerical damping and the initial conditions. In particular, if the system rotates very fast, the error can increase even of some orders of magnitude. In this condition, a good level of accuracy can be achieved only with very small time step sizes. However, the most systems for offshore wind energy purposes usually have low rotational speeds. The simulations of such systems can be performed using rather large time step sizes (for instance 0.05 s). The numerical damping, usually associated with a loss of energy, can increase the error but without significantly affecting the accuracy.

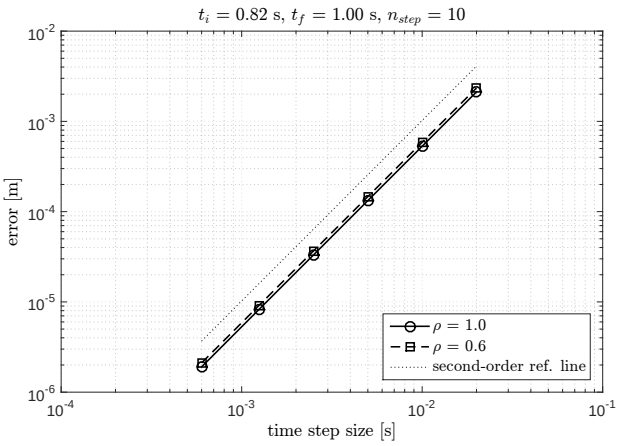

(a) error

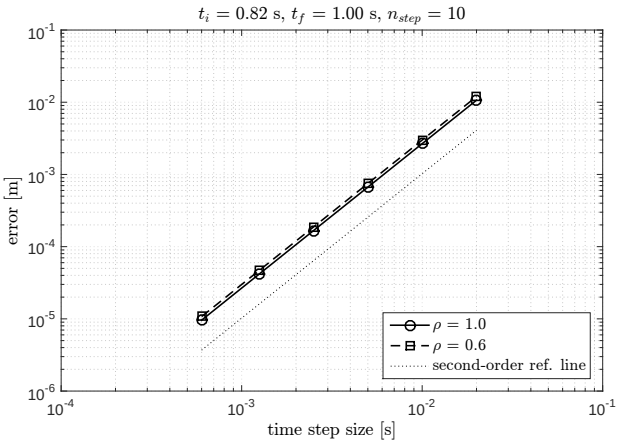

(b) error, initial velocity doubled

Figure 4: Axially symmetric rigid body: comparison between the numerical solution and the exact analytic solution.

7.3 Forced damped harmonic oscillator

Let's consider a rigid body with a linear spring and a linear damper connected to the center of mass and forced by a non-follower sinusoidal force, without any other external load (even the gravitational field is considered null), in the case of natural initial conditions. The features of system and loads are reported in Table 4. The particular initial and boundary conditions make the system translate along the x-axis without rotating, therefore the differential problem can be reduced to the study of a one-dimensional forced damped oscillator.

7.3.1 Analytic solution

In this case, the differential problem of a six d.o.f. rigid body can be reduced to a simple forced damped harmonic oscillator along the x-axis. The initial value problem is

environment		
gravity acceleration, g	0.00	m/s^2
rigid body		
mass, m	1.0	kg
natural frequency, ω_n	π	rad/s
damping factor, ν	0.3	-
loads		
stiffness, $A^{\mathbf{q}}_{11}$	$m\omega_n^2$	N/m
damping, $A^{\mathbf{v}}_{11}$	$2\nu\omega_n m$	N·s/m
force, $F^{nf}_{G,1}$	$\sin(2\omega_n t)$	N
initial conditions		
displacement, $\hat{q}_1\|_{t=0}$	0.0	m
velocity, $\hat{v}_1\|_{t=0}$	0.0	m/s

Table 4: Forced damped harmonic oscillator: parameters used for the analysis.

given by[19]:

$$m\ddot{x}_{G,1} + C^t_{11}\dot{x}_{G,1} + K^t_{11}x_{G,1} = F^{\mathcal{S}}_{G,1} = F\sin(\omega t) \quad (40)$$

$$x_{G,1}|_{t=0} = x_0 = 0, \quad \dot{x}_{G,1}|_{t=0} = \dot{x}_0 = 0 \quad (41)$$

The stiffness, the damping[20] and the mass of the system identify the natural angular frequency ω_n and the damping factor ν, namely:

$$\omega_n = \sqrt{\frac{K^t_{11}}{m}} \quad (42)$$

$$\nu = \frac{C^t_{11}}{2m\omega_n} \quad (43)$$

The exact analytic solution of the differential problem is given by:

$$\begin{aligned} x_{G,1} = {} & x^*\sin(\omega t - \psi) + \\ & - e^{-\nu\omega_n t}x^*\Big[\sin(-\psi)\cos(\omega_n\sqrt{1-\nu^2}t) + \\ & + \frac{\omega\cos(-\psi) + \nu\omega_n\sin(-\psi)}{\omega_n\sqrt{1-\nu^2}}\sin(\omega_n\sqrt{1-\nu^2}t)\Big] \end{aligned} \quad (44)$$

$$x^* = \frac{F}{K^t_{11}\sqrt{(1-\alpha^2)^2 + 4\nu^2\alpha^2}} \quad (45)$$

$$\mathrm{tg}\psi = \frac{2\nu\alpha}{1-\alpha^2}, \quad \alpha = \frac{\omega}{\omega_n} \quad (46)$$

[19]In order to not weigh the notation down, the indication of both reference frame and basis is omitted, namely:

$$\mathbf{x} = \mathbf{x}^{I,\mathcal{S}}$$

[20]The stiffness and the damping of the system can be modelled respectively as a linear transformation of the displacement, i.e. $K^t_{11} \equiv A^{\mathbf{q}}_{11}$, and as a linear transformation of the velocity, i.e. $C^t_{11} \equiv A^{\mathbf{v}}_{11}$. Since the body does not rotate, both non-follower and follower transformations can be used in the model.

7.3.2 Results

The numerical and analytic solutions are compared in terms of mean absolute error evaluated on the displacement of the center of mass $\mathbf{x}^{I,\mathcal{S}}_G$ at a set of specified times t_i, by using the Equation (38). The algorithm (see Figure 5(a)), as expected, has a second-order accuracy which is slightly influenced by the numerical damping, even if the error does not significantly change.

The trajectory of the center of mass (see Figure 5(b)), predicted by the time integrator, matches the exact analytic solution without any appreciable difference and, after an initial transient due to the initial conditions (homogeneous solution), the system is only driven by the forcing load (particular solution).

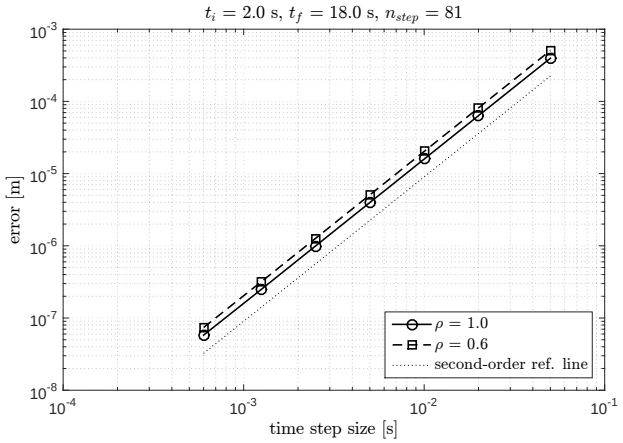

(a) error

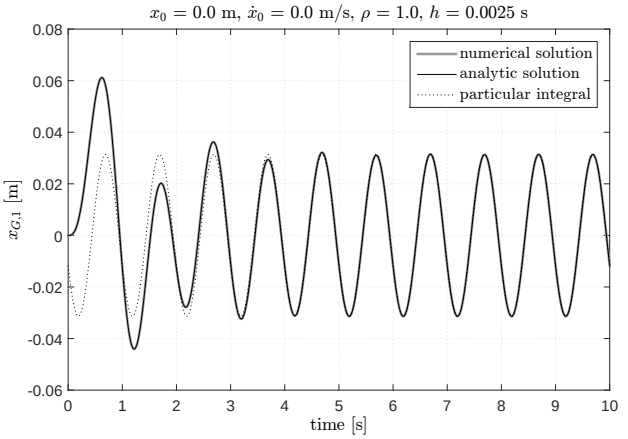

(b) trajectory

Figure 5: Forced damped harmonic oscillator: comparison between the numerical solution and the exact analytic solution.

7.3.3 Remarks

The time integrator can properly describe the motion of a translating body with a satisfying level of accuracy. The numerical damping, sometime necessary, can increase the error but without significantly compromising the accuracy.

7.4 Rigid body with follower loads

Let's consider a rigid body in the Euclidean space forced by a set of follower loads modelled as external sinusoidal force and torque and linear transformations of the state variables (displacement, velocity and acceleration vectors). The features of system and loads are illustrated in Table 5. An additional constant non-follower force is considered to balance the weight of the body (due to the gravitational field). In this section, the algorithm based on the spatial formulation is compared with the algorithms based on the mixed and local formulations[21].

environment		
gravity acc., g	9.81	m/s^2
rigid body		
mass, m	1.0	kg
inertia, $\mathbf{J}$	$m \cdot \mathrm{diag}(20\ 20\ 10)$	kg·m^2
loads		
stiffness, $\mathbf{B^q}$	$10^{-3}\mathrm{rand} - \mathrm{sym}(6,6)$	•
damping, $\mathbf{B^v}$	$10^{-3}\mathrm{rand} - \mathrm{sym}(6,6)$	•
inertia, $\mathbf{B^{\dot{v}}}$	$10^{-3}\mathrm{rand} - \mathrm{sym}(6,6)$	•
force, $\mathbf{F}^f$	$10^{-1}\sin(\pi/5 \cdot t)[1\ 0\ 0]^T$	N
force, $\mathbf{F}^{nf}$	$mg[0\ 0\ 1]^T$	N
torque, $\mathbf{T}^f$	$10^{-1}\sin(\pi/10 \cdot t)[0\ 1\ 0]^T$	N·m
initial conditions		
displ., $\hat{\mathbf{q}}\|_{t=0}$	$[0\ 0\ 0\ 0\ 0\ 0]^T$	m|rad
velocity, $\hat{\mathbf{v}}\|_{t=0}$	$[0\ 0\ 0\ 0\ 0\ 0]^T$	m/s|rad/s

Table 5: Rigid body with follower loads: parameters used for the analysis.

7.4.1 Results

The operators associated with the follower linear transformations of the state variables were randomly generated and converted into symmetric matrices simply by taking the mean value of the extra-diagonal terms, namely:

$$B_{ij}^{(\bullet)} = B_{ji}^{(\bullet)} = \frac{1}{2}(B_{ij}^{\mathrm{rand}} + B_{ji}^{\mathrm{rand}}) \qquad \text{for} \quad i \neq j \tag{47}$$

The operators used for the simulations are the following:

$$\mathbf{B^q} = 10^{-4}\begin{bmatrix} 7.69 & & & & & \\ 3.78 & 1.55 & & & sym & \\ 8.26 & 2.59 & 5.34 & & & \\ 0.00 & 0.00 & 0.00 & 0.00 & & \\ 0.00 & 0.00 & 0.00 & 0.00 & 0.00 & \\ 0.00 & 0.00 & 0.00 & 0.00 & 0.00 & 0.00 \end{bmatrix} \tag{48}$$

$$\mathbf{B^v} = 10^{-4}\begin{bmatrix} 3.48 & & & & & \\ 1.96 & 4.42 & & & sym & \\ 6.35 & 6.96 & 4.42 & & & \\ 2.66 & 2.78 & 4.21 & 4.30 & & \\ 4.07 & 5.67 & 5.70 & 8.21 & 3.77 & \\ 7.73 & 6.72 & 3.76 & 5.31 & 3.27 & 8.34 \end{bmatrix} \tag{49}$$

$$\mathbf{B^{\dot{v}}} = 10^{-4}\begin{bmatrix} 3.18 & & & & & \\ 3.32 & 6.47 & & & sym & \\ 5.79 & 3.25 & 1.10 & & & \\ 5.06 & 7.42 & 3.46 & 7.72 & & \\ 3.36 & 3.31 & 5.50 & 5.13 & 5.25 & \\ 7.50 & 7.39 & 4.21 & 8.22 & 6.36 & 5.20 \end{bmatrix} \tag{50}$$

The different algorithms (see Figure 6) predict the same trajectory of the center of mass as well as the same orientation of the body. The curves of the components of the rotational vectors have some discontinuities which occur when the magnitude of the rotation reaches the value of π rad because the algorithm is set up to return a magnitude in the interval $[-\pi,\ \pi]$. For this reason, for very large rotations it could be necessary to keep track of the actual rotation by adding (or subtracting) 2π rad to the module of the rotational vector whenever such a discontinuity occurs. However, note that the records of the velocities (see Figure 7) and accelerations are not affected by the discontinuities in the time history of the rotational vector.

7.4.2 Remarks

The algorithms based on the spatial, mixed and local formulations can be considered equivalent in terms of predicted motion of the body. However, as far as the computational effort is concerned, it should be properly investigated in order to better understand which formulation could guarantee the lesser computational effort.

[21] These algorithms have been implemented and validated in the aforementioned PhD research activity.

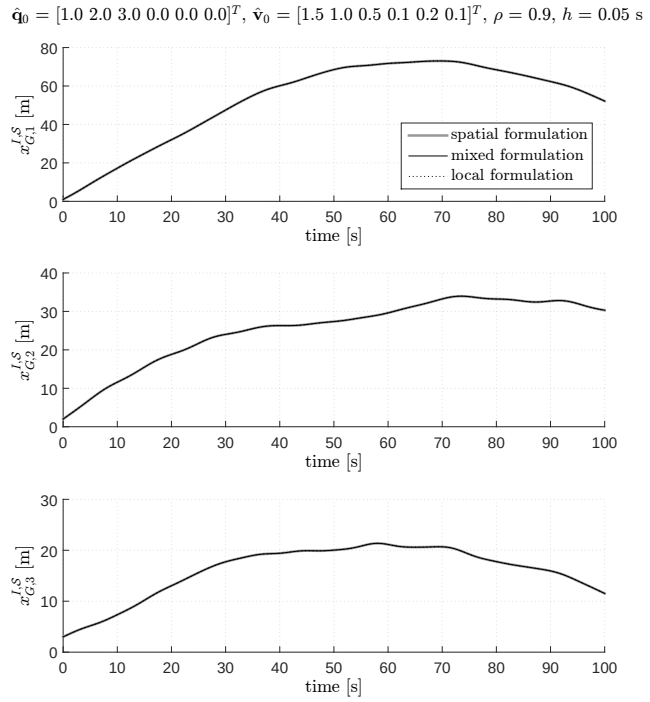

(a) trajectory of the center of mass

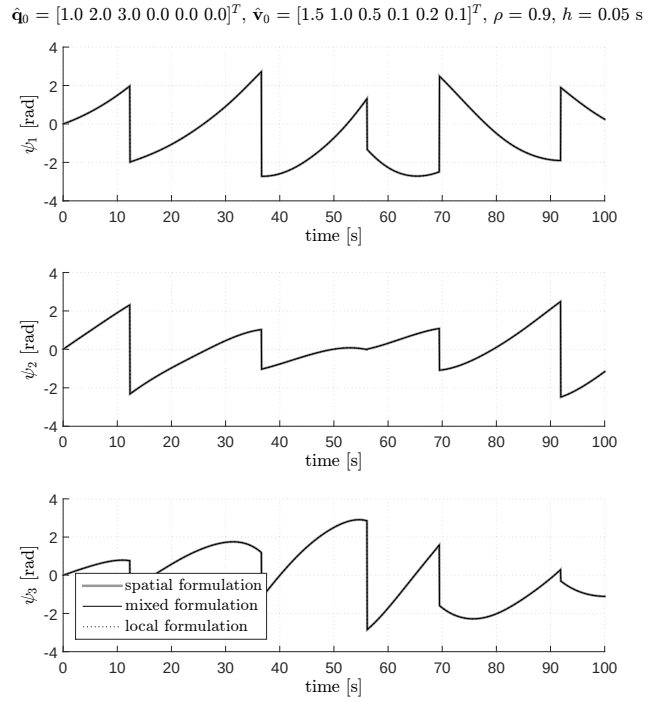

(b) orientation of the body

Figure 6: Rigid body with follower loads, configuration of the body: comparison between the numerical solutions obtained with the algorithms based on either the spatial formulation or the mixed formulation or the local formulation.

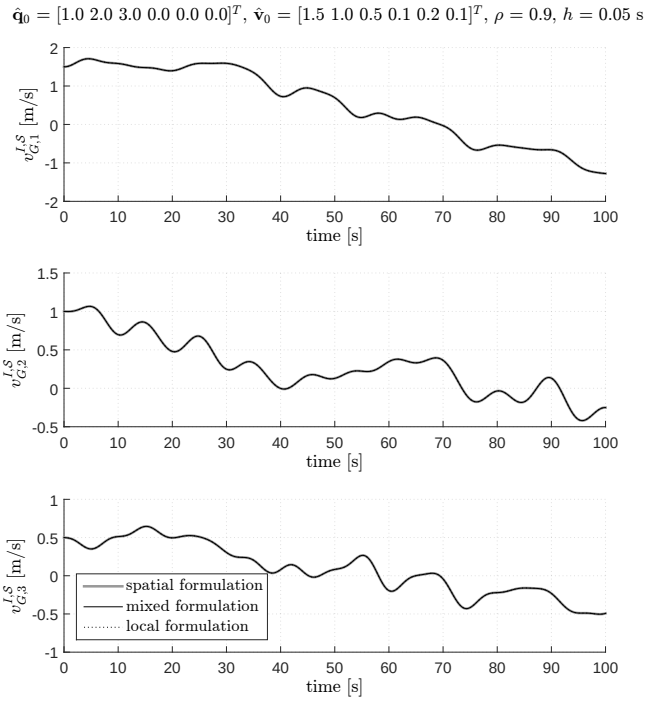

(a) velocity of the center of mass

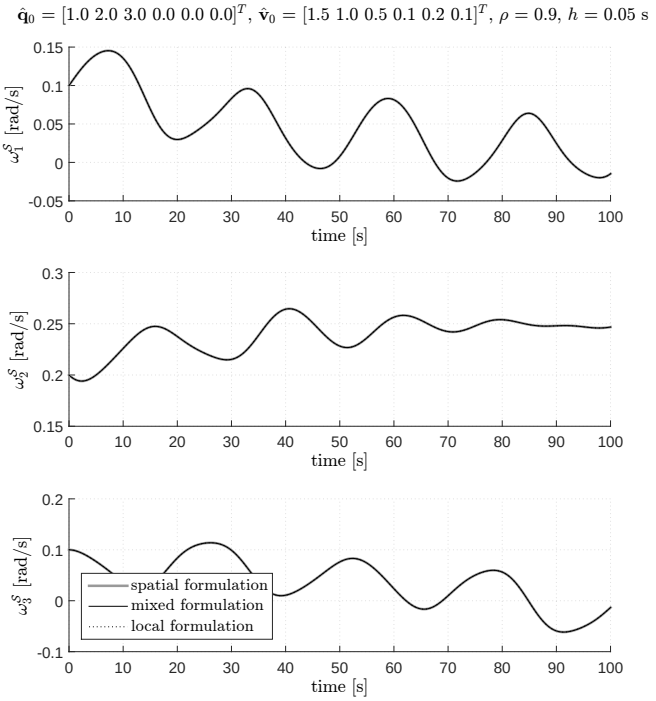

(b) angular velocity

Figure 7: Rigid body with follower loads, velocity of the body: comparison between the numerical solutions obtained with the algorithms based on either the spatial formulation or the mixed formulation or the local formulation.

References

[1] Brüls, O., Cardona, A.: On the use of Lie group time integrators in multibody dynamics. Journal of Computational and Nonlinear Dynamics **5** (2010)

[2] Brüls, O., Cardona, A., Arnold, M.: Numerical solution of DAEs in flexible multibody dynamics using lie group time integrators. In: The 1^{st} Joint International Conference on Multibody System Dynamics. Lappeenranta, Finland (2010)

[3] Brüls, O., Cardona, A., Arnold, M.: Two lie group formulations for dynamic multibody systems with large rotations. In: Proceedings of the ASME 2011 International Design Engineering Technical Conferences & Computers and Information in Engineering Conference. Washington, DC, USA (2011)

[4] Brüls, O., Cardona, A., Arnold, M.: Lie group generalized-α time integration of constrained flexible multibody systems. Mechanism and Machine Theory **48**, 121–137 (2012)

[5] Cardona, A., Geradin, M.: A beam finite element non-linear theory with finite rotation. International Journal for Numerical Methods in Engineering **26**, 2403–2438 (1988)

[6] Celledoni, E., Marthinsen, H., Owren, B.: An introduction to lie group integrators - basics, new developments and applications. Journal of Computation Physics **257**, 1040–1061 (2014)

[7] Celledoni, E., Owren, B.: Lie group methods for rigid body dynamics and time integation on manifolds. Computer Methods in Applied Mechanics and Engineering **192**, 421–438 (2003)

[8] Chung, J., Hulbert, G.M.: A time integration algorithm for structural dynamics with improved numerical dissipation: The generalized-α method. Journal of Applied Mechanics **60**, 371–375 (1993)

[9] EWEA: Wind in power, 2015 European statistics. Report, The European Wind Energy Association (2016)

[10] Géradin, M., Cardona, A.: Flexible Multibody Dynamics - A Finite Element Approach. John Wiley & Sons Ltd (2001)

[11] Jonkman, J., Matha, D.: A quantitative comparison of the responses of three floating platforms. Conference Paper NREL/CP-500-46726, National Renewable Energy Laboratory, Golden, Colorado (2010)

[12] Jonkman, J.M.: Dynamics of offshore floating wind turbines - model development and verification. Wind Energy **12**, 459–492 (2009)

[13] Mäkinen, J.: Critical study of newmark-scheme on manifold of finite rotations. Computer Methods in Applied Mechanics and Engineering **191**, 817–828 (2001)

[14] Müller, A., Terze, Z.: Geometric methods and formulations in computational multibody system dynamics. Acta Mechanica **227**, 3327–3350 (2016)

[15] Philippe, M., Babarit, A., Ferrant, P.: Modes of response of an offshore wind turbine with directional wind and waves. Renewable Energy **49**, 151–155 (2013)

[16] Romano, M.: Exact analytic solution for the rotation of a rigid body having spherical ellipsoid of inertia and subjected to a constant torque. Celestial Mechanics and Dynamical Astronomy **100**, 181–189 (2008). Online version with Errata Corrige

[17] Romano, M.: Exact analytic solutions for the rotation of an axially symmetric rigid body subjected to a constant torque. Celestial Mechanics and Dynamical Astronomy **101**, 375–390 (2008). Online version with Errata Corrige

[18] Simo, J.C.: A finite strain beam formulation. The three-dimensional dynamic problem. Part I. Computer Methods in Applied Mechanics and Engineering **49**, 55–70 (1985)

[19] Simo, J.C., Vu-Quoc, L.: A three-dimensional finite-strain rod model. Part II: computational aspects. Computer Methods in Applied Mechanics and Engineering **58**, 79–116 (1986)

[20] Simo, J.C., Vu-Quoc, L.: On the dynamics in space of rods undergoing large motions - a geometrically exact approach. Computer Methods in Applied Mechanics and Engineering **66**, 125–161 (1988)

[21] Sonneville, V.: A geometric local frame approach for flexible multibody systems. PhD dissertation (2015). Université de Liège, Aerospace and Mechanical Engineering Department, Multibody and Mechatronic Systems Lab

[22] Sonneville, V., Cardona, A., Brüls, O.: Geometrically exact beam finite element formulated on the special Euclidean group SE(3). Computer methods in applied mechanics and engineering **268**, 451–474 (2014)

[23] Terze, Z., Zlatar, D., Müller, A.: Numerical integration algorithm in Lie-group setting for dynamics of mechanical systems. In: Proceedings of 7th International Congress of Croatian Society of Mechanics (7ICCSM 2012). Zadar, Croatia (2012)